DOI: 10.1002/cbic.200800021

Tyl1a, a TDP-6-deoxy-D-*xylo*-4-hexulose 3,4-isomerase from *Streptomyces fradiae*: Structure Prediction, Mutagenesis and Solvent Isotope Incorporation Experiments to Investigate Reaction Mechanism

Mónica Tello,[a, b] Martin Rejzek,[a, b] Barrie Wilkinson,[c] David M. Lawson,*[b] and Robert A. Field*[a, b]

Understanding the structure and mechanism of sugar nucleotide processing enzymes is invaluable in the generation of designer enzymes for biotransformation, for instance, in connection with engineering antibiotic glycosylation. In this study, homology modelling and mechanistic comparison to the structurally related RmlC epimerase family has been used to identify and assign functions to active-site residues in the Tyl1a-catalysed keto-sugar nucleotide isomerisation process. Tyl1a His63 is implicated as the base that initiates the isomerisation process by substrate C-3 deprotonation, with Arg109 stabilising the resulting enolate. Subsequent O-3 deprotonation (potentially by His65) and C-4 protonation (potentially by Tyr49) complete the isomerisation process.

Introduction

The keto-sugar nucleotide TDP-6-deoxy-D-*xylo*-4-hexulose is a common and versatile biosynthetic intermediate that is enzymatically elaborated in a number of ways. For instance, it serves as a precursor to all three sugar nucleotide units required for decoration of the tylactone core en route to the macrolide antibiotic tylosin (Scheme 1).[1] On a broader front, TDP-6-deoxy-D-*xylo*-4-hexulose is also used in nature as an intermediate en route to a variety of different sugars, including 3-acetamido-3-deoxy-D-fucose (via TDP-6-deoxy-D-*xylo*-3-hexulose)[2] and L-rhamnose (via TDP-6-deoxy-L-*lyxo*-4-hexulose;[3,4] Scheme 1). Our interest was drawn to the little studied *Streptomyces fradiae* TDP-6-deoxy-D-*xylo*-4-hexulose 3,4-ketoisomerase, Tyl1a, which participates in the biosynthesis of TDP-D-mycaminose. Examination of the tylosin biosynthetic gene cluster coupled with heterologous expression experiments highlighted a previously unassigned open reading frame, subsequently named *tyl1a*, directly upstream of *tylB*.[5,6] Expression of *tyl1a* in *Streptomyces venezuelae* along with genes previously assigned a role in mycaminose biosynthesis enabled the successful reconstitution of the entire mycaminose pathway, and supported the notion that *tyl1a* encodes an essential TDP-6-deoxy-D-*xylo*-4-hexulose 3,4-isomerase capable of forming TDP-6-deoxy-D-*ribo*-3-hexulose.[6] More recently, in vitro studies with recombinant Tyl1a protein have confirmed its function;[7] further, a homologue of Tyl1a, QdtA from *Thermoanaerobacterium thermosaccharolyticum* E207-71, has recently been characterised.[8]

Analysis of the Tyl1a sequence[7] has shown that it is a member of the cupin superfamily,[9] from which the keto-sugar nucleotide epimerase RmlC is the most studied member.[10,11] Our laboratory has a long-standing interest in the structure and mechanism of such sugar nucleotide epimerases.[12–16] Given the number of examples of enzymes that operate on the same substrate as Tyl1a (Figure 1), we were prompted to investigate the mechanism of Tyl1a action. Previous studies on the Tyl1a homologue, FdtA, noted that it contained no common motifs with other known isomerase families and that it might act by a novel mechanism.[2] The absence of metal-binding or oxido-reductase cofactor binding motifs suggests that Tyl1a- and FdtA-catalysed isomerisation processes (Scheme 1) might proceed via enolate chemistry, in a similar manner to the epimerisation reactions catalyzed by RmlC (vide supra).[13] Initially in the absence of structural information for Tyl1a, we generated models based on crystallographic data for the weakly homologous RmlC family. These models, together with sequence alignment information and consideration of residues involved in the RmlC action, were used to guide site-directed mutagenesis of Tyl1a in order to identify active-site residues involved in its mechanism of action. Towards the conclusion of our study, the crystal structure of keto-sugar nucleotide isomerase FdtA was reported.[17] The studies reported herein support and extend observations and mechanistic proposals for substrate isomerisation based on the FdtA structure. In particular, experiments that employ solvent isotope incorporation have allowed us to establish and dissect the contribution of

[a] *Dr. M. Tello, Dr. M. Rejzek, Prof. Dr. R. A. Field*
School of Chemical Sciences and Pharmacy
University of East Anglia
Norwich, NR4 7TJ (UK)

[b] *Dr. M. Tello, Dr. M. Rejzek, Dr. D. M. Lawson, Prof. Dr. R. A. Field*
Department of Biological Chemistry, John Innes Centre
Colney Lane, Norwich, NR4 7UH (UK)
Fax: (+44) 1603 450018
E-mail: david.lawson@bbsrc.ac.uk
rob.field@bbsrc.ac.uk

[c] *Dr. B. Wilkinson*
Biotica, Chesterford Research Park
Saffron Walden CB10 1XL (UK)

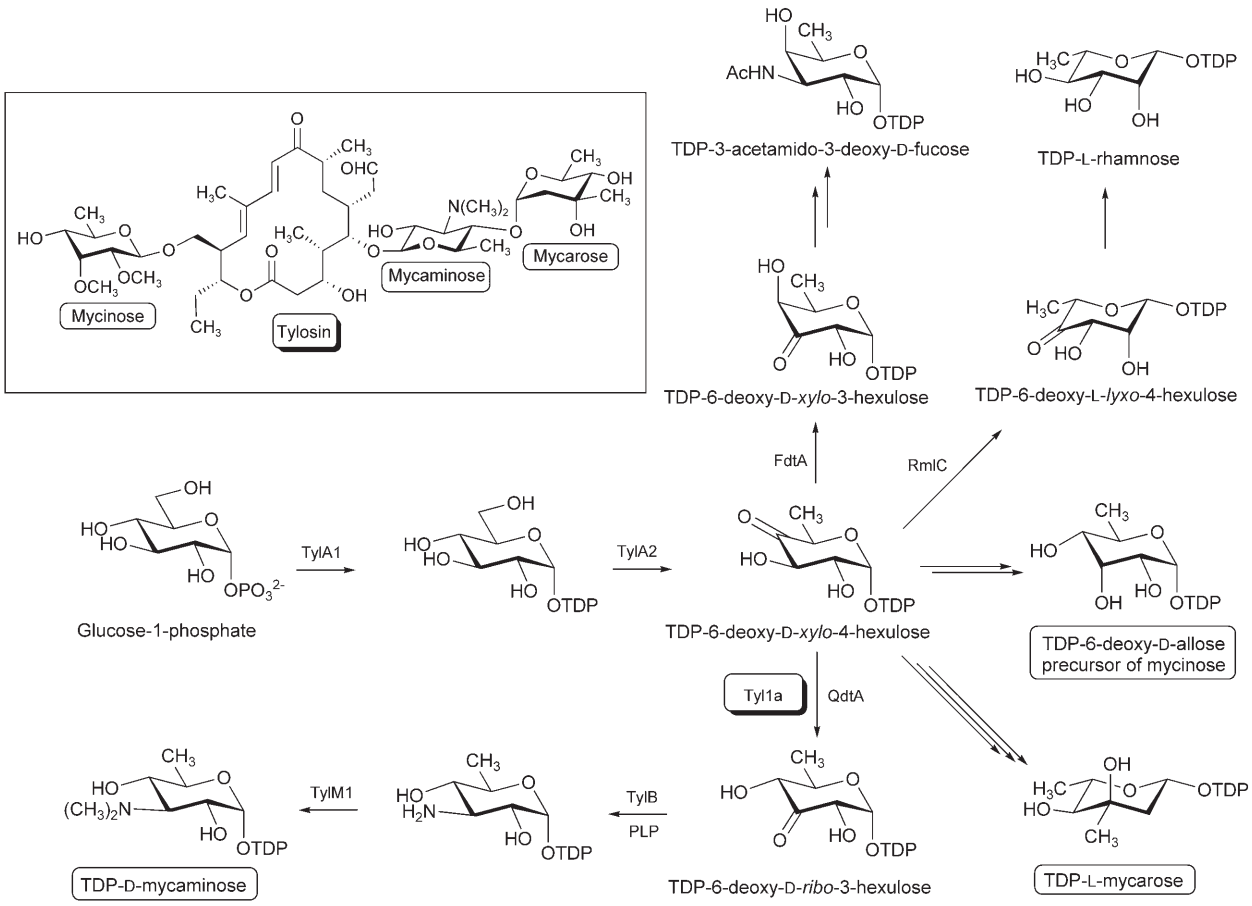

Scheme 1. The versatility of TDP-6-deoxy-D-*xylo*-4-hexulose as a biosynthetic building block and its relevance to tylosin biosynthesis.

putative active-site acids and bases; these studies have identified mechanistic similarities to the RmlC family of keto-sugar nucleotide epimerases.

Results

In silico studies

Comparison of RmlC family epimerases and putative Tyl1a family isomerases: Although the sequence identities between Tyl1a and RmlC proteins are of the order of 20% or less, we were drawn to consider potential similarities between Tyl1a and RmlC based on the potential for elements of common reaction mechanism. We, therefore, focussed our attention on the residues that have been implicated in substrate binding and in effecting the epimerisation process in RmlC that are also conserved in Tyl1a.

Residues involved in substrate binding: In the RmlC family, an active-site Arg residue (Arg60 in the *Salmonella* sequence; Figure 1) forms a hydrogen bond to the phosphate groups of the substrate[12] and in NovW to a sulfate molecule present in the active site of the substrate-free enzyme.[15] This Arg residue is located in the first position of an RGXH motif that is conserved in the broader RmlC-related family of epimerases and isomerases, which includes the Tyl1a, FdtA and QdtA isomerases (Figure 1). This suggested a common role for Arg60 in substrate binding and highlighted Tyl1a Arg60 for further investigation.

Residues involved in catalysis: The RmlC-catalysed 3,5-epimerisation of TDP-6-deoxy-D-*xylo*-4-hexulose is thought to proceed by initial epimerisation at C-5 followed by epimerisation at C-3,[13] as demonstrated for GDP-mannose epimerase (GME).[20] In the RmlC reaction, the axial proton at C-5 of the keto sugar is abstracted by a basic residue, His63, with subsequent formation of an enolate. This process is aided by stabilisation of the developing enolate by the surrounding positively charged residues, in particular the protonated side chain of Lys73, which lies in close proximity to the enolate oxyanion. The epimerisation process proceeds by proton transfer to C-5 from an acidic residue, Tyr133, located on the opposite face of the enolate to the original position of the H-5 proton. Subsequently, the H-3 proton is abstracted, which results in enolate formation and, on this occasion, protonation by water completes the second epimerisation reaction (Scheme 2).

When the Tyl1a sequence is aligned with the RmlC family, the catalytic His63 of RmlC aligns with His63 of Tyl1a (Figure 1). Indeed, the RGXH motif characteristic of the RmlC family, in which His is the catalytic base, is conserved in the

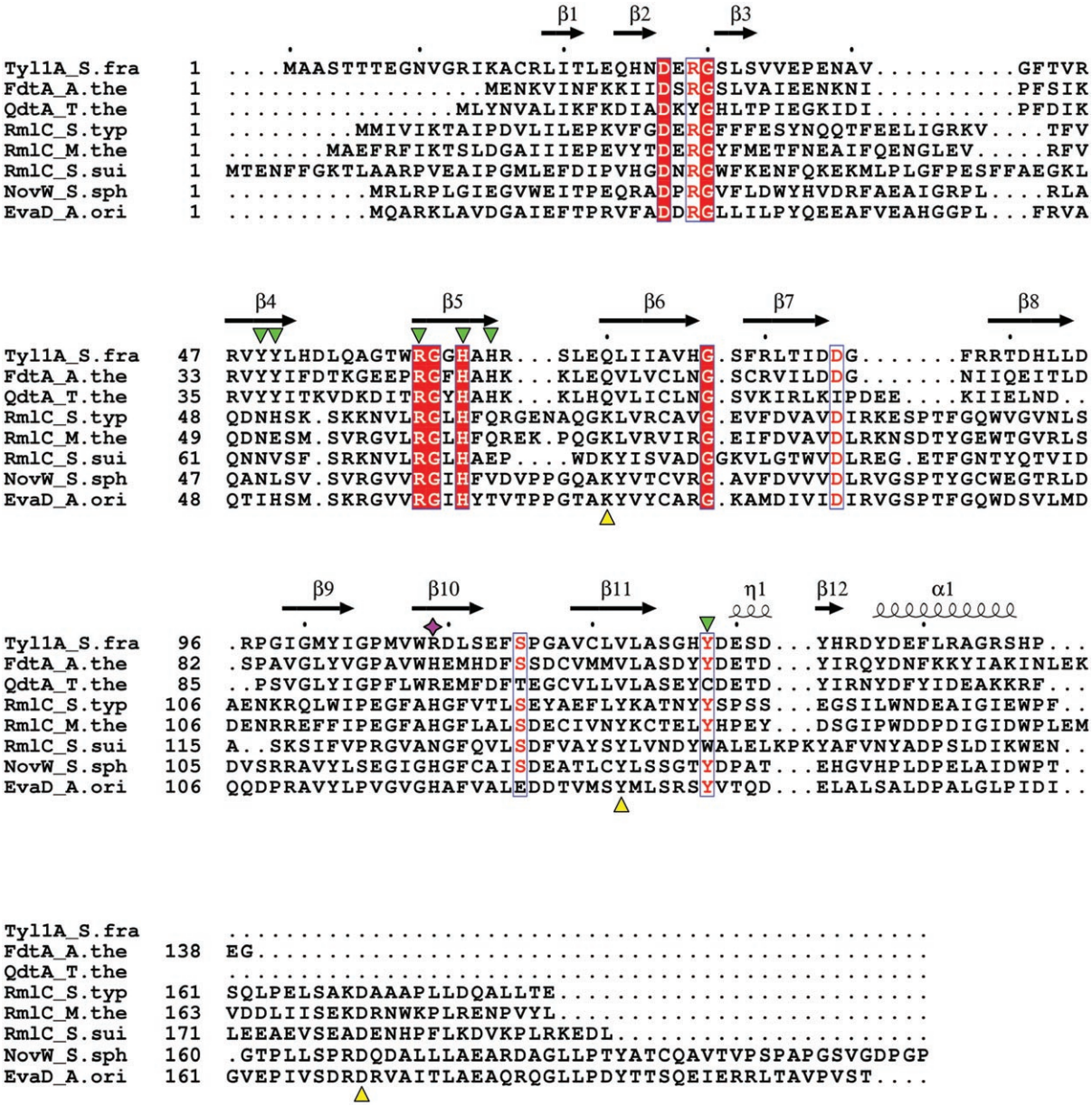

Figure 1. Structure-based multiple sequence alignment of *Streptomyces fradiae* Tyl1a (Tyl1a_S.fra) with selected isomerase and epimerase sequences displayed by using ESPript.[18] The initial alignment was generated by using EXPRESSO,[19] and subsequently adjusted manually with reference to superposed known structures. Strictly conserved residues are highlighted with red boxes, and well-conserved residues are boxed with the predominant residues in red. Secondary-structure elements for the Tyl1a homology model are shown above the alignment, where α helices are represented by an α, β strands by β and 3_{10} helices by η. Isomerases: FdtA from *Aneurinibacillus thermoaerophilus* (FdtA_A.the), QdtA from *Thermoanaerobacterium thermosaccharolyticum* (QdtA_T.the). Epimerases: RmlC from *Salmonella typhimurium* (RmlC_S.typ), RmlC from *Methanobacterium thermoautotrophicum* (RmlC_M.the), RmlC from *Streptococcus suis* (RmlC_S.sui), NovW from *Streptomyces spheroides* (NovW_S.sph), EvaD from *Amycalotopsis orientalis* (EvaD_A.ori). The residues mutated in this study are indicated by green triangles. Yellow triangles show the epimerase active-site residues His63 (base), Lys73 (enolate stabiliser), Tyr133 (acid) and Asp170 (dyad with His63; *S. typhimurium* sequence numbering). The purple star highlights Arg109 of Tyl1a that corresponds to His95 of FdtA (His in the RmlC family, as part of a second largely conserved His–Asp dyad, to which a precise function has not been assigned).

Tyl1a sequence. However, none of the remaining essential three catalytic residues of RmlC is conserved in Tyl1a—that is, Lys73 (stabilises enolate), Tyr133 (acid for first epimerisation), Asp170 (dyad with His63; *Salmonella* sequence numbering). This analysis highlighted Tyl1a His63 for further investigation.

Sequence analysis of Tyl1a and putative isomerase proteins: In attempting to identify possible candidates that might act as basic and acidic residues in the Tyl1a-catalysed isomerisation process, sequence alignments highlighted similarities between Tyl1a and several other proteins, including FdtA, which is an experimentally validated 3,4-isomerase from *Aneurinibacillus thermoaerophilus* (sequence identity to Tyl1a 34%) that forms TDP-6-deoxy-D-*xylo*-3-hexulose from TDP-6-deoxy-D-*xylo*-4-hexulose, and QdtA, which is an experimentally validated 3,4-isomerase from *T. thermosaccharolyticum* (sequence identity to

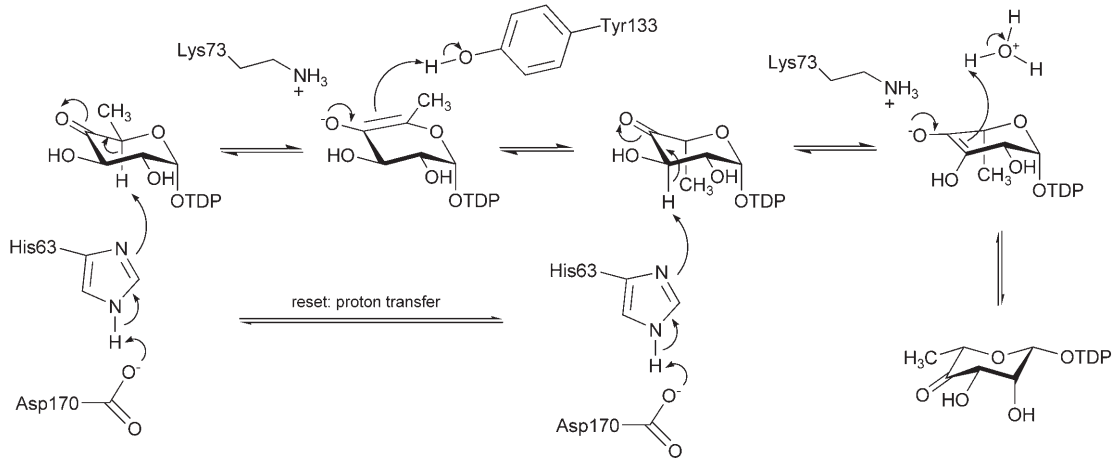

Scheme 2. The proposed mechanism of epimerisation catalysed by RmlC.

Tyl1a 33%) that forms TDP-6-deoxy-D-*ribo*-3-hexulose from TDP-6-deoxy-D-*xylo*-4-hexulose (Figure 1).[2,8] Two obvious motifs are evident in these three proteins. An acidic RRVYY motif (Tyl1a residues 46–50) is matched by KRVYY in FdtA and QdtA; the first residue is not conserved as such—both arginine and lysine possess the ability to support a positive charge through protonation. The first four amino acids of a conserved RGXHAH motif (Tyl1a residues 60–65) are described above in connection with a substrate binding Arg residue (first position of the motif) and the likely catalytic base (His in the fourth position of the motif). These alignment data highlighted Tyl1a Tyr49, Tyr50 and His65 for further investigation, and reinforced a likely functional role for His63. As a control, we also selected Tyl1a Tyr128, a tyrosine residue that is present in many epimerase and isomerase family sequences (Figure 1), but which is not directly involved in the mechanism of the former.

Generation of 3D models of wild-type Tyl1a: Ahead of mutagenesis studies on the residues already outlined (Tyl1a Tyr49, Tyr50, His63, His65, Arg60 and Tyr128), the plausibility of such residues being located in the active site of Tyl1a was considered. Due to the lack of relevant isomerase crystal structures when this study was initiated, homology models of Tyl1a based on the structurally characterised RmlC family were generated by using the 3D-PSSM[21] and FUGUE[22] fold recognition servers. The 3D-PSSM server generated a model based on RmlC from *Methanobacterium thermoautotrophicum* (PDB code 1EP0; sequence identity to Tyl1a 19%), and FUGUE used RmlC from *Salmonella typhimurium* (PDB code 1DZR; sequence identity to Tyl1a 14%) to produce a model. These models gave a similar disposition of the target residues around the cupin β-barrel fold, with one notable exception: in the 3D-PSSM model, Tyr49 pointed into the β barrel and Tyr50 pointed away from the β barrel, whereas in the FUGUE model, the opposite was true (models not shown). However, during the course of our work the crystal structure of FdtA from *A. thermoaerophilus* was published[17] (PDB ID code 2PA7; sequence identity to Tyl1a 34%). This was clearly a superior structure to use as a template for modelling Tyl1a. We, therefore, retrospectively generated a new model based on this structure using a combination of FUGUE (with *Z* score 26.7) and MODELLER[23] (Figure 2). This was comparable to both previous models, but was closest to the 3D-PSSM model with Tyr49 pointing into the β barrel and Tyr50 pointing away from the β barrel.

The structural analysis of FdtA potentially implicates His95 in substrate binding and/or catalysis. This residue is replaced by Arg in both Tyl1a (residue 109) and QdtA (residue 97). The corresponding residue forms part of a His–Asp dyad in some RmlCs, but no function has been assigned to this second dyad and indeed it is absent in the *Streptococcus suis* sequence. Combined, the lack of conservation of sequence and the absence of precedent for function did not encourage us to investigate this residue further at this stage.

In summary, the modelling confirmed that the residues we had highlighted based on sequence alignment data and mechanistic considerations were still valid targets for mutagenesis. We, therefore, decided to make the following Tyl1a mutants: Arg60Ala, His63Ala, His65Ala, Tyr49Phe, Tyr50Phe and Tyr128Phe.

Generation and characterisation of recombinant wild-type and mutant proteins

Cloning, over-expression and purification of wild-type Tyl1a: The 447 bp *tyl1a* gene was amplified from *S. fradiae* genomic DNA and cloned into pUC18.[5] This was subcloned into pET151/D-TOPO vector by using the pET directional TOPO cloning protocol in order to allow over-expression of the Tyl1a protein with a TEV-cleavable N-terminal His-tag. Tyl1a over-expression in *E. coli* BL21 (DE3) yielded high amounts of soluble and active protein (~25 mg L^{-1}), which was purified by nickel affinity chromatography and subsequently by size-exclusion chromatography to give highly pure material, as judged by SDS-PAGE.

Preparation, over-expression and purification of Tyl1a mutants: Tyl1a Tyr49Phe, Tyr50Phe, Arg60Ala, His63Ala, His65Ala and Tyr128Phe mutants were prepared by site-directed mutagenesis by using the QuickChange® mutagenesis protocol. Plasmids were then transformed into *E. coli* BL21 (DE3) and the mutant

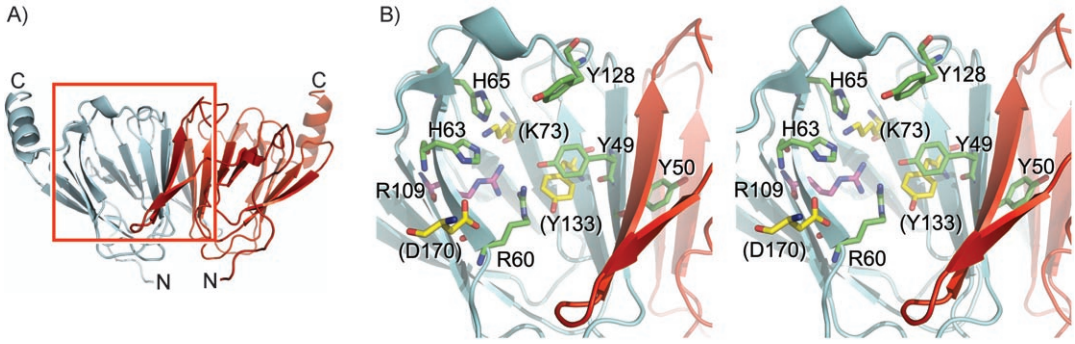

Figure 2. Homology model of Tyl1a based on the crystal structure of FdtA from *Aneurinibacillus thermoaerophilus* (PDB ID code: 2PA7). A) Tyl1a is likely to exist as a homodimer, in agreement with FdtA and epimerases in general, and has been modelled as such; this is depicted in cartoon representation. B) Stereo view looking into the mouth of one of the cupin β barrels of the homodimer (this corresponds to the red boxed region in A). The barrel is largely made up by β strands from one subunit (pale blue), but also contains two β strands donated from the neighbouring subunit (red). Residues selected for mutagenesis are shown with green carbon atoms. For reference, key active-site residues from RmlC that have no equivalents in Tyl1a are also shown in yellow (these are taken from the *S. typhimurium* structure, PDB ID code 1DZR, with the corresponding numbering in parentheses). Arg109, shown with purple carbons, is structurally equivalent to His95 of FdtA. The figure was generated by using PyMOL (http://www.pymol.org).

proteins were over-expressed in the same way as the wild type. The Tyr49Phe and His65Ala mutants yielded a very small amount of soluble protein, whereas Arg60Ala and His63Ala produced similar amounts to the wild type. In order to solve this problem, coexpression with the GroESL chaperone system[24] was employed where necessary. For instance, use of the GroESL system with the Tyr94Phe mutant resulted in an improvement of soluble expression of at least tenfold—that is, it gave an expression level comparable to the wild-type sequence expressed in the absence of GroESL. The mutant proteins were purified by nickel affinity chromatography and size-exclusion chromatography in a similar way to the wild-type protein.

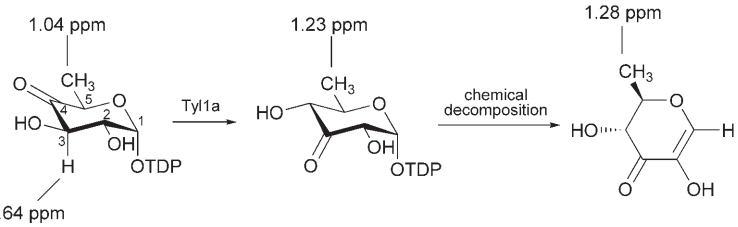

Scheme 3. Characteristic ^{1}H NMR signals used to monitor the Tyl1a-catalysed isomerisation of TDP-6-deoxy-D-*xylo*-4-hexulose to TDP-6-deoxy-D-*ribo*-3-hexulose and its subsequent chemical degradation. (The signals identified are for the hydrated ketones in the sugar nucleotides.)

^{1}H NMR enzyme-activity assay: The activity of Tyl1a proteins was assessed by ^{1}H NMR spectroscopy.[2,5] The Tyl1a substrate, TDP-6-deoxy-D-*xylo*-4-hexulose, was prepared enzymatically on a multimilligram scale by the action of recombinant RmlB on TDP-glucose.[25] In aqueous solution, the 4-keto starting material and 3-keto product exist predominantly (>75%) in the hydrated *gem*-diol form, which is spectroscopically distinct from the parent keto form. All reference herein is to these hydrates. For the purposes of the discussion, key signals used in our studies are identified in Scheme 3; NMR signals and protocols are in accord with those reported previously.[7]

Upon incubation of TDP-6-deoxy-D-*xylo*-4-hexulose (4-keto compound) with Tyl1a, formation of TDP-6-deoxy-D-*ribo*-3-hexulose (3-keto compound) was observed from the appearance of the clearly identifiable H-6 signal (amongst others). The signals corresponding to the 3-keto product progressively increased in parallel with reduction of the corresponding signals of the starting material. However, as noted by Liu and co-workers,[7] the formation of the 3-keto compound reaches a maximum at ~35% conversion, after which it slowly decomposes into a third compound, 2,3-dihydro-3,5-dihydroxy-2-methyl-4-pyrone. The appearance of decomposition product following formation of the TDP-6-deoxy-D-*xylo*-3-hexulose was earlier reported in a FdtA-catalysed reaction.[2] The competing chemical degradation of the Tyl1a reaction product potentially complicates the quantitative kinetic analysis of the Tyl1a-catalysed isomerisation of TDP-6-deoxy-D-*xylo*-4-hexulose. We, therefore, resorted to the direct analysis of both substrate depletion and product formation by ^{1}H NMR spectroscopy in D_2O, which allowed the isomerisation catalysed by Tyl1a, and mutants thereof, to be followed. This approach enabled us to assess the relative rates of deuterium incorporation into substrate and the rate of substrate isomerisation, which offers potential to dissect the overall isomerisation process.[1]

Characterisation of wild-type Tyl1a: The rate of Tyl1a-catalysed reaction was monitored by analysing the changes in intensity of ^{1}H NMR signals characteristic of the TDP-6-deoxy-D-*xylo*-4-hexulose substrate and TDP-6-deoxy-D-*ribo*-3-hexulose product (Table 1). For the wild-type Tyl1a reaction, the rate of appearance of the H-6 signal for the 3-keto compound was slightly lower than the rate of disappearance of the H-6 signal of the starting 4-keto compound due to competing degradation of the former to 2,3-dihydro-3,5-dihydroxy-2-methyl-4-pyrone. In addition, these studies showed a faster rate (two-

[1] *^{1}H NMR spectroscopy data for TDP-6-deoxy-D-xylo-4-hexulose, the product TDP-6-deoxy-D-ribo-3-hexulose and the resulting chemical degradation product 2,3-dihydro-3,5-dihydroxy-2-methyl-4-pyrone were in accordance with literature data; this allows for differences that result from different buffers and reference standards.*[2,7,8,25]

Table 1. Initial rates of reaction (nmol s^{-1}) of Tyl1a wild type (WT) and mutants based on changes in ^{1}H NMR signal intensities for the methyl group (H-6; decrease at 1.04 ppm) and the H-3 proton (decrease at 3.64 ppm) of TDP-6-deoxy-D-*xylo*-4-hexulose, along with an increase in signal intensity of the methyl group of the isomerised product TDP-6-deoxy-D-*ribo*-3-hexulose product (H-6; increase at 1.23 ppm).

NMR signal[a,b] / Tyl1a protein	WT	Arg60Ala	His63Ala	His65Ala	Tyr49Phe	Tyr50Phe	Tyr128Phe
substrate / H-6	−0.55	−0.11	n.d.	n.d.	n.d.	−0.44	−0.45
product / H-6	+0.50	+0.05	n.d.	n.d.	n.d.	+0.42	+0.39
substrate / H-3	−1.24	−0.16	n.d.	−1.21	−1.43	−0.91	−1.20

[a] n.d.: not detectable; [b] experimental error about ±5%.

fold) of removal of the C-3 proton than of isomerisation (based on the rate of change in signal intensity of the substrate and product C-5 methyl groups). This observation is consistent with a stepwise rather than a concerted isomerisation process.

Discussion and Conclusion

In the absence of a metal-ion cofactor, the chemistry required for Tyl1a action encouraged us to consider an RmlC-like acid/base mechanism.[12] A combination of sequence alignment and an homology model generated from the FdtA crystal structure suggested that Tyr49, Arg60, His63 and His65 all point towards the inside of the β barrel that forms the Tyl1a active site and create a binding pocket to accommodate the keto-sugar nucleotide substrate. This drove the rational choice of residues for mutagenesis: Arg60Ala, His63Ala, His65Ala, Tyr49Phe, Tyr50Phe and Tyr128Phe. Following ^{1}H NMR characterisation of the reaction catalysed by the six mutants, the lack of effect on reaction rates suggested that Tyr50 and Tyr128 are not involved in Tyl1a-catalysed keto-sugar nucleotide isomerisation. The other mutants gave reduced rates or only partial reactions; this result enables speculation about the contribution of each amino acid to steps in the isomerisation process.

Characterisation of Tyl1a (wild-type sequence): It is interesting to note that for Tyl1a the rate of deuterium incorporation at C-3 was faster than the generation of isomerised product; this is consistent with H-3 deprotonation occurring before the rate-determining step.

Characterisation of Tyl1a Arg60Ala: The Arg60Ala-catalysed reaction showed very slow substrate isomerisation (approx five- to tenfold slower than wild type) with appearance of the signals that corresponded to both the 3-keto compound and decomposition product after a few hours of incubation at 37 °C. This suggests that Arg60 plays a supporting role in the Tyl1a reaction, and most likely plays a role in substrate binding, as is the case for the corresponding residue in RmlC (discussed in ref. [13]) and evident in the crystal structure of the FdtA-TDP co-complex.[17]

Characterisation of His63Ala and His65Ala: Isomerised 3-keto compound or decomposition product were not detected in reactions with the His63Ala mutant, even after several days of incubation at 37 °C. In contrast, His65Ala showed a wild-type reaction rate for removal of the C-3 proton. However, formation of the 3-keto product and decomposition product was drastically slowed down: after overnight incubation, only moderate (~20%) formation of the decomposition product was evident, with no sign of the 3-keto isomerisation product. Presence of the decomposition product clearly indicates that there was formation of TDP-6-deoxy-D-*xylo*-3-hexulose, but its rate of formation proved slower than its chemical decomposition. Along with sequence alignment with the catalytic base from RmlC,[13] and in keeping with mutagenesis studies on FdtA,[17] these results strongly implicate Tyl1a His63 in the initial H-3 abstraction. Interestingly, in the Tyl1a family isomerases, this basic histidine residue appears to operate on its own. In contrast, in the RmlC epimerase family the corresponding histidine is located in a conserved His–Asp dyad. In the appropriate *S. suis* RmlC Asp-to-Ala mutant, k_{cat}/K_m is lower by ~130-fold compared to the wild-type protein, but the K_m remains essentially unchanged.[26] The precise requirement for the dyad is unclear, but it could be associated with resetting the ionisation state of the base for the requisite second round of C–H deprotonation during the RmlC-catalysed double 3,5-epimerisation reaction. This might suggest that in Tyl1a, His63 is required for only a single deprotonation step.

Analysis of Tyl1a His65Ala shows a normal rate of deuterium incorporation at C-3; this confirms that it is *not* the basic residue that initiates the isomerisation reaction. However, the dramatic reduction in His65Ala isomerase activity (as judged by the lack of detectable change on the H-6 signals of substrate and product) suggests that it plays a role later in the Tyl1a-catalysed isomerisation process. Again, the reduced isomerase activity of this mutant is consistent with data for the corresponding FdtA mutant.[17] [2]

Characterisation of Tyr49Phe, Tyr50Phe and Tyr128Phe: These mutants were aimed at identifying catalytic acid residues that participate in the keto-isomerisation process. In the case of Tyr50Phe and Tyr128Phe, the rate of the isomerisation reaction was similar to the wild type. Mutation of these two Tyr residues did not affect the enzyme activity; this suggests that these residues are not directly involved in the isomerisation process. In the case of Tyr49Phe, only disappearance of the substrate H-3 proton signal was observed, at a similar rate to the wild type (Table 1), and no other notable changes were evident. This indicated that this mutation had affected the reaction after removal of the H-3 proton, and implicated Tyl1a Tyr49 as an essential residue for activity. This residue likely plays a role as an acid in the keto-isomerisation process, perhaps by protonating an enol/enolate intermediate at the sugar

[2] *Any differences can be attributed to the fact that the Tyl1a mutations were to Ala, whereas the FdtA mutations were to Asn.*

C-4 in a manner analogous to that of the key active-site tyrosine residues in the RmlC and EvaD epimerases, which protonate an enolate intermediate at the sugar C-5 position in order to complete the C-5 epimerisation process.

Putative mechanism of the Tyl1a-catalysed ketoisomerisation reaction: It is clear that Tyl1a His63 initiates isomerisation of TDP-6-deoxy-D-*xylo*-4-hexulose by deprotonating C-3 of the keto sugar. This step is directly analogous to the first step in epimerisaton (of the same substrate) catalysed by the RmlC family. However, in the latter a conserved lysine residue serves to stabilise the oxyanion of the enolate; in Tyl1a the corresponding residue is Arg109, whilst in FdtA it is His95—a residue that has been considered to have a potential role in catalysis.[17] Given the demonstrated requirement for His65 in both Tyl1a and FdtA action, it is conceivable that this residue serves to deprotonate the 3-OH group of the enolate intermediate in order to drive isomerisation, with concomitant C-4 protonation by Tyr49 to complete the process to give TDP-6-deoxy-D-*ribo*-3-hexulose (Scheme 4).

Given the likelihood of a common mechanism up to the C-protonation step, this putative mechanism leaves the question of how Tyl1a and FdtA are able to generate stereoisomeric products from a common enolate intermediate—that is, C-4 equatorial alcohol for Tyl1a (C-4 axial alcohol for FdtA). As with the ambiguity in the mechanism of RmlC family epimerases,[13,14] one is left to conclude that subtleties in the orientation of either (or both) active-site side chains and the enolate intermediate might account for the difference in stereochemical outcome of the Tyl1a- and FdtA-catalysed isomerisation reactions.

Experimental Section

Cloning of Tyl1a: The 447 bp *tyl1a* gene was amplified from *S. fradiae* genomic DNA by using the primers 5′-GGGCATATGAACGACCGTCCCCGCCGCGCCATGAAGGG-3′ and 5′-CCCCTCTAGAGGTCACTGTGCCCGGCTGTCGGCGGCGGCCCCGCGCATGG-3′, and cloned into pUC18.[5] For over-expression of the corresponding protein with a TEV-cleavable N-terminal His-tag, the *tyl1a* gene was subcloned into pET151/D-TOPO vector by using the pET directional TOPO cloning protocol (Invitrogen). TOP10 competent cells were transformed with the resulting plasmid, and single colonies were isolated and cultured to generate plasmid stocks by using a miniprep kit (Qiagen).

Over-expression of Tyl1a: The plasmid was transformed into *E. coli* BL21 (DE3), a single colony was selected and grown for 8 h at 37 °C in LB media (5 mL, containing 100 μg mL^{-1} ampicillin). A sample of this culture (0.5 mL) was used to inoculate a seed culture (50 mL of LB media with 100 μg mL^{-1} of ampicillin, incubated at 37 °C, overnight), which in turn was used to inoculate a production culture (1 L of LB media, 100 μg mL^{-1} of ampicillin) that was incubated at 37 °C until the OD_{600} reached 0.5–0.6. At that point, the culture was induced with IPTG (final concentration 0.4 mM) and was shaken at 37 °C for 4–5 h. The cells were harvested by centrifugation (13000 *g* for 10 min) and were stored at −20 °C until required.

Purification of Tyl1a and mutants: The cell pellet stock was resuspended in Tris buffer (10 mL; 50 mM, pH 8.0, 300 mM NaCl, 10 mM imidazole). Cells were lysed by passing the suspension three times through a French press and the membranes were centrifuged (33000 *g* for 30 min). The supernatant was loaded onto a nickel HiTrap chelating column (5 mL; Amersham) that was pre-equilibrated with buffer (50 mM Tris, pH 8.0, 300 mM NaCl, 20 mM imidazole). The column was then washed with five column volumes (CV) of the same buffer to elute unspecifically bound proteins. A gradient from 0–75% of elution buffer (50 mM Tris, pH 8.0, 500 mM NaCl, 500 mM imidazole) in 10 CV followed by a 75–100% in 10 CV was applied for the elution of Tyl1a. The fractions collected, as well as the flow-through and cell pellet, were analysed by SDS-PAGE gel. Those fractions containing Tyl1a were pooled and dialysed at 4 °C, overnight (against 2 L of 20 mM Tris, pH 8.0, 150 mM NaCl). The protein was then loaded on a HiLoad™ Superdex™ 16/60 column (Amersham) that was equilibrated with 2 CV of the dialysis buffer. The fractions containing Tyl1a were pooled and concentrated to ~5 mg mL^{-1}. The protein was flash-frozen in liquid nitrogen, with no requirement of cryoprotection, prior to storage at −80 °C. Tyl1a was stable upon thawing of the samples without reduction of activity.

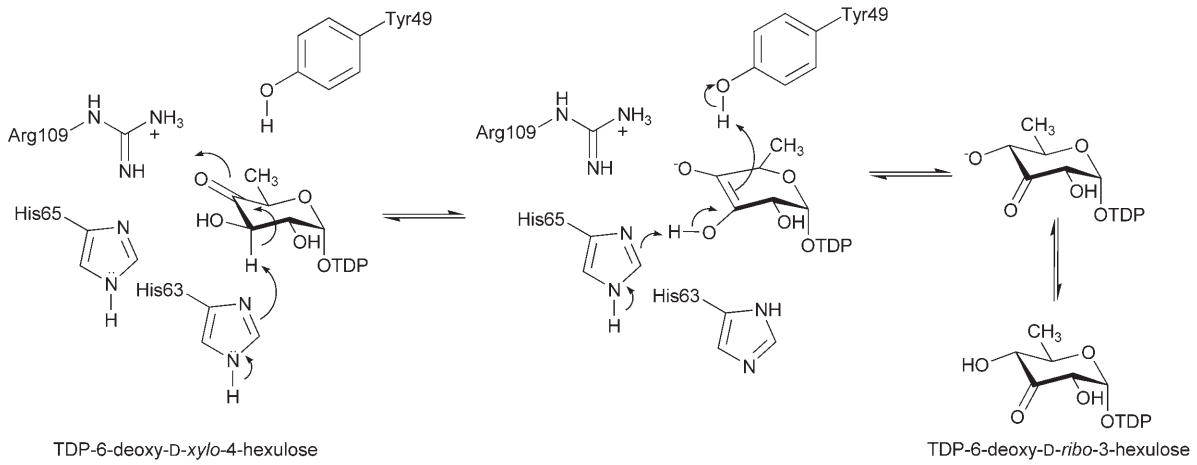

Scheme 4. Putative mechanism of Tyl1a-catalysed isomerisation of TDP-6-deoxy-D-*xylo*-4-hexulose to TDP-6-deoxy-D-*ribo*-3-hexulose. The final alkoxide protonation can be performed either by the enzyme or water.

Site-directed mutagenesis: Tyl1a mutants were prepared by using the principle of QuickChange® mutagenesis (Stratagene). The primers used to generate Tyl1a mutants are listed in Table 2. The PCR

Table 2. Sequence of the primers used for *tyl1a* mutagenesis.

	Primer sequence (5′→3′)
Tyr49Phe forward	C GTG CGG CGC GTG TTC TAC CTG CAC GAT CTG C
Tyr49Phe reverse	G CAG ATC GTG CAG GTA GAA CAC GCG CCG CAC G
Tyr50Phe forward	GTG CGG CGC GTG TAC TTC CTG CAC GAT CTG CAG
Tyr50Phe reverse	CTG CAG ATC GTG CAG GAA GTA CAC GCG CCG CAC
Arg60Ala forward	GCC GGC ACC TGG GCC GGC GGA CAC GCC
Arg60Ala reverse	GGC GTG TCC GCC GGC CCA GGT GCC GGC
His63Ala forward	C TGG CGC GGC GGA GCC GCC CAC CGC TCT C
His63Ala reverse	G AGA GCG GTG GGC GGC TCC GCC GCG CCA G
His65Ala forward	GGC GGA CAC GCC GCC CGC TCT CTG GAG
His65Ala reverse	CTC CAG AGA GCG GGC GGC GTG TCC GCC
Tyr128Phe forward	CTG GCC TCG GGG CAC TTC GAC GAG TCG GAC TAC C
Tyr128Phe reverse	G GTA GTC CGA CTC GTC GAA GTG CCC CGA GGC CAG

reactions for mutagenesis experiments were prepared as follows: DNA template (1 μL), Kod polymerase (1 μL of 1 U μL^{-1}), polymerase buffer (5 μL of 10× stock), dNTP mix (8 μL of 2 mM), forward primer (2 μL of 10 μM), reverse primer (2 μL of 10 μM), $MgSO_4$ (3 μL of 25 mM) and MilliQ water (28 μL). After PCR the reactions were incubated with DpnI restriction enzyme (10 U) for 2 h and transformed into DH5α competent cells. The plasmid stocks isolated from single DH5α colonies were sequenced to check the presence of the correct mutation.

Preparation of TDP-6-deoxy-D-*xylo*-4-hexulose: TDP-glucose (20 mg, 33 μmol) was incubated with RmlB (3 mg)[25] and NADH (1 mM) in sodium phosphate buffer (2 mL of 20 mM, pH 7.6) at 37 °C for 20 h. Protein was removed by filtration through a Centriprep concentrator (4 mL; Amicon), the filtrate was lyophilized and stored at −20 °C until required.

^{1}H NMR activity assays: Enzymes used in NMR spectroscopy assays were prepared by being exchanged into a deuterated buffer (50 mM NaD_2PO_4 in D_2O, pD 7.5) by using Centricon spin filters with a 10 kDa cut-off. Enzymatic reactions were performed as follows: TDP-6-deoxy-D-*xylo*-4-hexulose (2 mg) was dissolved into D_2O (0.7 mL; substrate concentration 5 μM) at 37 °C, a spectrum of the starting material was acquired and the reaction was initiated by the addition of Tyl1a (50 μg; final assay concentration ~3 μM). Spectra were recorded at intervals over a period of ~2–24 h, depending on the rate of reaction. NMR signals and protocols are in accord with those reported previously.[7]

Acknowledgements

These studies were supported by a Norwich Research Park Studentship (M.T.) and EPSRC grant GR/S820046/01 (M.R.). Work in the Lawson laboratory was supported by the BBSRC through responsive mode funding (ref B19400) and the Core Strategic Grant to the John Innes Centre. We thank Prof. Jim Naismith (University of St. Andrews) for helpful discussions. Dr. Colin MacDonald and Dr. Shirley Fairhurst, and Dr. Lionel Hill are thanked for invaluable assistance with NMR spectroscopy and mass spectrometry, respectively. Dr. Sabine Gaisser (Biotica) is acknowledged for supply of the original Tyl1a clone.

Keywords: antibiotics · enzyme catalysis · isomerases · structure analysis · sugar nucleotides

[1] E. Cundliffe, N. Bate, A. Butler, S. Fish, A. Gandecha, L. Merson-Davies, *Antonie Van Leeuwenhoek* **2001**, *79*, 229.
[2] A. Pfoestl, A. Hofinger, P. Kosma, P. Messner, *J. Biol. Chem.* **2003**, *278*, 26410.
[3] M. Graninger, B. Nidetzky, D. E. Heinrichs, C. Whitfield, P. Messner, *J. Biol. Chem.* **1999**, *274*, 25069.
[4] R. J. Stern, T. Y. Lee, T. J. Lee, W. Yan, M. S. Scherman, V. D. Vissa, S. K. Kim, B. L. Wanner, M. R. McNeil, *Microbiology* **1999**, *145*, 663.
[5] S. Gaisser, PCT WO054 265, **2005**.
[6] C. E. Melancon, W. L. Yu, H.-w. Liu, *J. Am. Chem. Soc.* **2005**, *127*, 12240.
[7] C. E. Melancon, L. Hong, J. A. White, Y. N. Liu, H.-w. Liu, *Biochemistry* **2007**, *46*, 577.
[8] A. Pföstl, S. Zayni, A. Hofinger, P. Kosma, C. Schäffer, P. Messner, *Biochem. J.* **2008**, *410*, 187.
[9] S. Khuri, F. T. Bakker, J. M. Dunwell, *Mol. Biol. Evol.* **2001**, *18*, 593.
[10] S. T. Allard, M. F. Giraud, J. H. Naismith, *Cell. Mol. Life Sci.* **2001**, *58*, 1650.
[11] R. A. Field, J. H. Naismith, *Biochemistry* **2003**, *42*, 7637.
[12] M. F. Giraud, G. A. Leonard, R. A. Field, C. Berlind, J. H. Naismith, *Nat. Struct. Biol.* **2000**, *7*, 398.
[13] C. J. Dong, L. L. Major, V. Srikannathasan, J. C. Errey, M. F. Giraud, J. S. Lam, M. Graninger, P. Messner, M. McNeil, R. A. Field, C. Whitfield, J. H. Naismith, *J. Mol. Biol.* **2007**, *365*, 146.
[14] A. B. Merkel, L. L. Major, J. C. Errey, M. D. Burkart, R. A. Field, C. T. Walsh, J. H. Naismith, *J. Biol. Chem.* **2004**, *279*, 32684.
[15] P. Jakimowicz, M. Tello, C. L. Meyers, C. T. Walsh, M. J. Buttner, R. A. Field, D. M. Lawson, *Proteins Struct. Funct. Bioinf.* **2006**, *63*, 261.
[16] M. Tello, P. Jakimowicz, J. C. Errey, C. L. Freel Meyers, C. T. Walsh, M. J. Buttner, D. M. Lawson, R. A. Field, *Chem. Commun.* **2006**, 1079.
[17] M. L. Davis, J. B. Thoden, H. M. Holden, *J. Biol. Chem.* **2007**, *282*, 19227.
[18] P. Gouet, E. Courcelle, D. I. Stuart, F. Metoz, *Bioinformatics* **1999**, *15*, 305.
[19] F. Armougom, S. Moretti, O. Poirot, S. Audic, P. Dumas, B. Schaeli, V. Keduas, C. Notredame, *Nucleic Acids Res.* **2006**, *34*, W604.
[20] L. L. Major, B. A. Wolucka, J. H. Naismith, *J. Am. Chem. Soc.* **2005**, *127*, 18309.
[21] L. A. Kelley, R. M. MacCallum, M. J. Sternberg, *J. Mol. Biol.* **2000**, *299*, 501.
[22] J. Shi, T. L. Blundell, K. Mizuguchi, *J. Mol. Biol.* **2001**, *310*, 243.
[23] A. Sali, T. L. Blundell, *J. Mol. Biol.* **1993**, *234*, 779.
[24] I. E. Ichetovkin, G. Abramochkin, T. E. Schrader, *J. Biol. Chem.* **1997**, *272*, 33009.
[25] A. Naundorf, W. Klaffke, *Carbohydr. Res.* **1996**, *285*, 141.
[26] C. J. Dong, L. L. Major, A. Allen, W. Blankenfeldt, D. J. Maskell, J. H. Naismith, *Structure* **2003**, *11*, 715.

Received: January 12, 2008
Published online on April 21, 2008

